SF2A 2011
G. Alecian, K. Belkacem, R. Samadi and D. Valls-Gabaud (eds)

PLANETARY MIGRATION IN WEAKLY MAGNETIZED TURBULENT DISCS

C. Baruteau[1], S. Fromang[2], R. P. Nelson[3] and F. Masset[4]

Abstract. In laminar viscous disc models, the migration of protoplanets embedded in their nascent protoplanetary discs may be directed inwards or outwards, depending on the relative magnitude of the Lindblad and corotation torques. The long-term evolution of the corotation torque is intimately related to diffusion processes inside the planet's horseshoe region. This communication examines the properties of the corotation torque in discs where magnetohydrodynamic (MHD) turbulence develops as a result of the magnetorotational instability (MRI), considering a weak initial toroidal magnetic field. We show that the differential Lindblad torque takes very similar values in MHD turbulent and laminar viscous discs, and there exists an unsaturated corotation torque in MHD turbulent discs.

Keywords: accretion discs, magnetohydrodynamics (MHD), turbulence, methods: numerical, planetary systems: planet-disc interactions , planetary systems: protoplanetary discs

1 Introduction

By combining models of planetary formation and migration, and models of protoplanetary discs, planet population syntheses (e.g., Ida & Lin 2008; Mordasini et al. 2009) have shown that the reproduction of the mass-period diagram of known exoplanets is particularly sensitive to the magnitude of the tidal torque driving the migration of forming protoplanets, known as type I migration. The latter has been intensively studied in two-dimensional (2D) non-magnetized, laminar viscous disc models. In such models, the tidal torque comprises the differential Lindblad torque and the corotation torque. The differential Lindblad torque corresponds to the angular momentum carried away by the spiral density waves the planet generates in the disc (see illustration in Fig. 1). Alone, it would drive type I migration on timescales typically $\leq 10^5$ yrs, shorter than the timescale for giant planet formation (e.g., Ward 1997). The corotation torque corresponds to the exchange of angular momentum between the planet and the fluid elements inside its horseshoe region. The magnitude of the corotation torque is powered by advection-diffusion of gas vortensity and entropy inside the horseshoe region. Alone, it would drive migration inwards or outwards, depending on the background density and temperature profiles.

A lot of efforts have been recently put forward to derive simple and accurate expressions for the Lindblad and corotation torques (Masset & Casoli 2010; Paardekooper et al. 2011). The question that we address here is to what extent these predictions, which are based on viscous disc models, still hold in the presence of MHD turbulence arising from the MRI, a likely source of turbulence in protoplanetary discs.

2 Physical model and numerical setup

We explore the properties of the tidal torque between a planet and its nascent protoplanetary disc, wherein turbulence is driven by the non-linear development of the MRI. The key point we address is whether an unsaturated corotation torque exists and can be maintained in the long term in such turbulent discs. For this purpose, we performed 3D MHD simulations with the Nirvana and Ramses codes, adopting a simple disc model with a locally isothermal equation of state, and neglecting non-ideal MHD effects as well as vertical stratification.

---

[1] DAMTP, University of Cambridge, Wilberforce Road, Cambridge CB30WA, United Kingdom

[2] Laboratoire AIM, CEA/DSM-CNRS-Université Paris Diderot, IRFU/SAp, CEA/Saclay, 91191 Gif-sur-Yvette, France

[3] Astronomy Unit, Queen Mary University of London, Mile End Road, London E1 4NS, United Kingdom

[4] Instituto de Ciencias Físicas, Universidad Nacional Autónoma de México, Apdo. Postal 48-3, 62251-Cuernavaca, Morelos, México

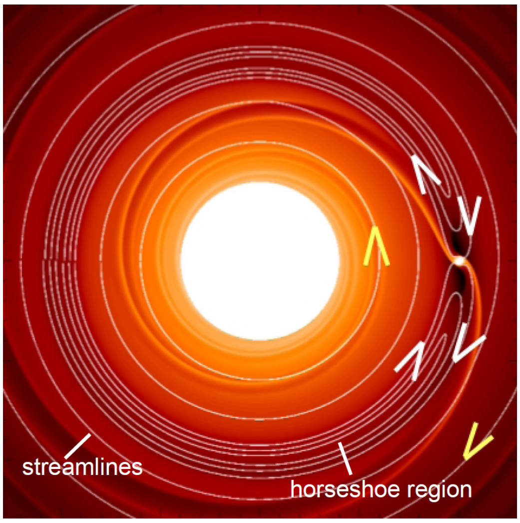

Fig. 1. Disc density perturbed by a few Earth-mass planet. Streamlines in the frame corotating with the planet are overplotted by solid curves.

Table 1. Disc, grid and planet parameters used in the MHD simulations

Parameter	Value	Remarks
Radial resolution	320 cells in $R \in [1;8]$	
Azimuthal resolution	480 cells in $\varphi \in [0;\pi]$	15-20 cells per H at planet location
Vertical resolution	40 cells in $z \in [-0.3;0.3]$	
Initial magnetic field	Toroidal, set up in $R \in [1.5;5]$	
Plasma β-parameter	$\beta = 50$ (Nirvana), $\beta = 400$ (Ramses)	
Aspect ratio	$h = H/R = 0.1$ at $R = 3$	
Planet mass	$M_{\rm p} = 3 \times 10^{-4} M_\star$	$M_{\rm p}/(h^3 M_\star) = 0.3$ at planet location
Planet location	$R_{\rm p} = 3, \varphi_{\rm p} = \pi/2, z_{\rm p} = 0$	(planet subject to type I migration)
Planet's softening length	$\varepsilon = 0.2H(R_{\rm p})$	
Frame	Corotating with $R = R_{\rm p}$	
Radial boundary condition	Wave-killing zones in $R \in [1;1.5]$ and $R \in [7;8]$	

No explicit kinematic viscosity is included. When included, the planet remains on a fixed circular orbit, and the tidal torque exerted by the disc on the planet is measured as a time series. To get a steady-state density profile, the initial density profile is reinforced on 20 planet orbits. The key parameters used in the simulations are summarized in Table 1. For more details about the numerical setup, the reader is referred to Baruteau et al. (2011). For comparison, results with 2D viscous disc models without magnetic field, having otherwise the same disc and planet parameters as in the 3D MHD models are also presented below.

3 Results of simulations

3.1 *Disc model with an inner cavity (planet trap)*

In locally isothermal discs, the corotation torque can be particularly large in disc regions where the density gradient is positive, and for this reason we performed a sequence of simulations with the planet located in a turbulent disc with an inner cavity. The planet orbits in the transition region between the outer high-density disc and the inner low-density cavity, a region often referred to as a planet trap (Masset et al. 2006). The sequence was initiated with a preliminary viscous 1D run aimed at obtaining a steady-state density profile with an inner cavity. This run was used to construct a 3D cylindrical disc model into which a purely toroidal magnetic field was introduced throughout the disc. This magnetized disc model was evolved until MHD turbulence was fully developed before inserting the planet.

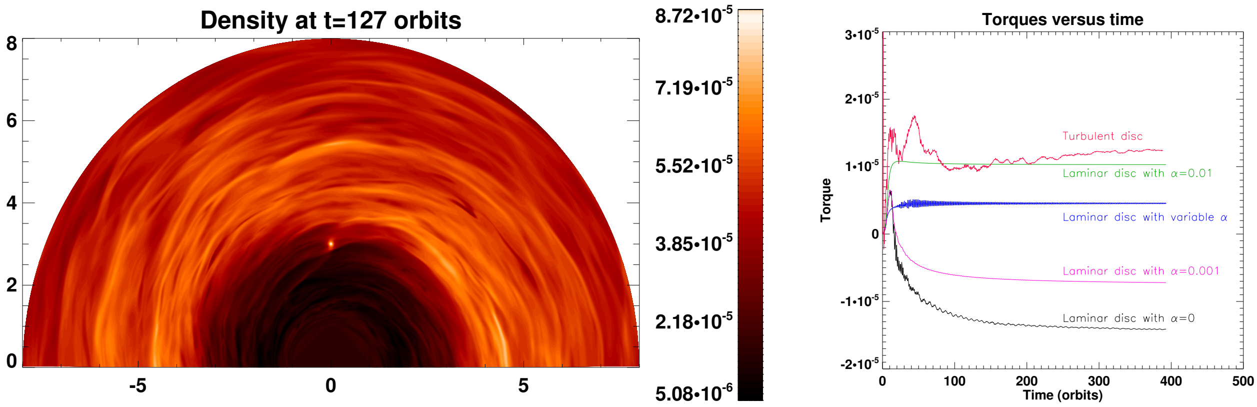

Fig. 2. Left: disc midplane density obtained with the cavity run of § 3.1. The planet is located at $x = 0$, $y = 3$. Right: running time-averaged torque obtained with the turbulent cavity model. Torques of laminar disc models with similar density profile and various viscosities at the planet location are superimposed for comparison.

The disc's midplane density obtained 127 orbits after the planet insertion is displayed in the left panel of Fig. 2, where we can see the planet sitting at the edge of the cavity. The time-averaged alpha viscous parameter associated with the turbulent stress is $\langle\alpha\rangle \approx 0.02$ near the planet. The running time-average of the torque exerted by the disc on the planet is shown by the red curve in the right panel of Fig. 2. The results of 2D laminar simulations with different viscosities are depicted for comparison. The time-averaged turbulent torque remains positive, indicating that the corotation torque is sustained at a value close to its maximum, unsaturated value throughout the simulation. These results strongly suggest that a planet trap maintained in a turbulent protoplanetary disc can be effective in preventing the large scale migration of embedded protoplanets.

3.2 Disc models with a power-law density

To provide a more quantitative comparison between the results of MHD turbulent and viscous disc models, we consider in this section two disc models where the initial profiles of the disc density (ρ_0) and temperature (T_0) are power-law functions of radius. In Model 1, $\rho_0 \propto R^{-1/2}$ and $T_0 \propto R^{-1}$. In Model 2, $\rho_0 \propto R^{-3/2}$ and T_0 is uniform. In the absence of magnetic field and turbulence, the corotation torque would vanish in Model 2, but not in Model 1. Although it is uncertain how a toroidal magnetic field modifies the dependence of the corotation torque with density and temperature gradients, the tidal torque values obtained in both models can hint whether MHD turbulence impacts the differential Lindblad torque and the corotation torque.

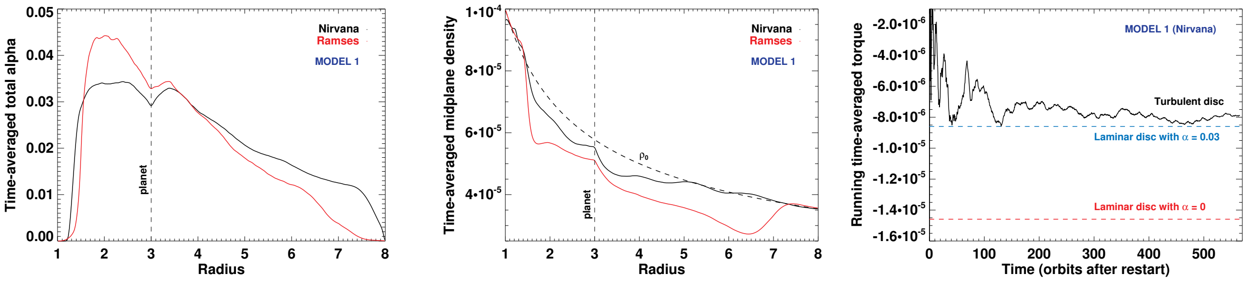

Fig. 3. Results obtained with disc Model 1 in § 3.2: radial profiles of the alpha viscous parameter (left) and midplane density (middle), time-averaged over 100 orbits. Right: Running time-averaged torque. The stationary torques of 2D non-magnetized laminar disc models (inviscid and viscous) are overplotted, in which the profiles of ρ_0 and α correspond to their time-averaged MHD counterpart.

The key results obtained with Model 1 are summarized in Fig. 3. The left panel shows the time-averaged profile of the total alpha viscous parameter obtained with both codes. At the planet location, $\langle\alpha\rangle \sim 0.03$, a value that translates into an averaged diffusion timescale across the planet's horseshoe region that is slightly longer than the horseshoe U-turn timescale. The corotation torque is thus expected to adopt a value close to that predicted by linear theory. The middle panel displays the azimuthally- and time-averaged disc midplane density. The fact the initial density is restored over 20 local orbital periods implies that we get a stationary density profile slightly reduced compared to the initial one, depicted by a dashed curve. The right panel shows the running time-averaged turbulent torque, along with the final torque obtained in 2D inviscid ($\alpha = 0$) and viscous ($\alpha = 0.03$) non-magnetic disc models. The running time-averaged turbulent torque reaches a stationary value after $\sim$ 200 orbits, and is in decent agreement with the torque of the laminar disc model with similar viscous alpha parameter near the planet. Although not shown here, similar results were obtained with Model 2, as well as a remarkably good overall agreement between the results of both codes.

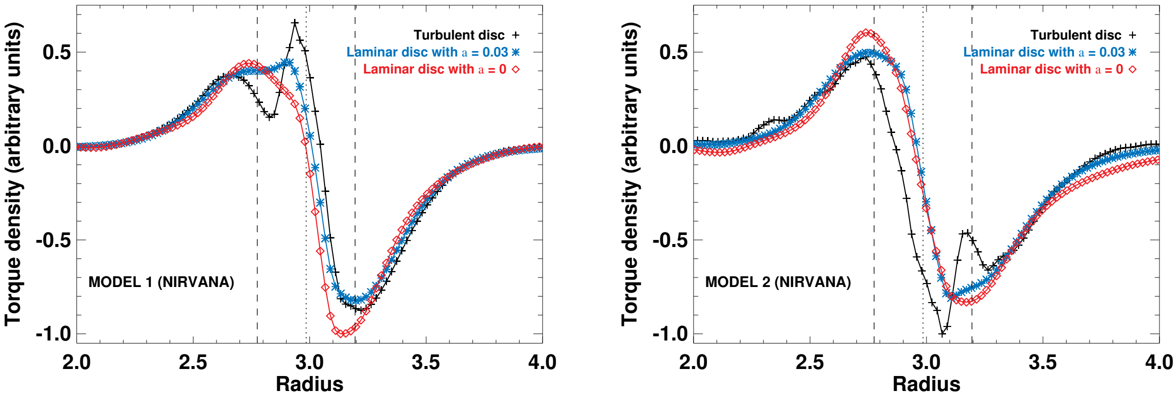

Fig. 4. Torque density distribution time-averaged over 100 orbits. The (stationary) torque distributions of inviscid and viscous disc models are overplotted. The dashed lines show the approximate location of the separatrices of the planet's horseshoe region.

To gain insight into the similar torque values of the turbulent and viscous disc models, we show in Fig. 4 the time-averaged torque distribution of the turbulent torque, and the stationary torque distribution of the inviscid and viscous models. The planet is located at $R = 3$ and the vertical dashed lines show the approximate location of the separatrices of its horseshoe region. We see that outside the horseshoe region, the very good agreement between the turbulent and laminar torque distributions shows that, on time average, the differential Lindblad torque is essentially unchanged by the full development of MHD turbulence. Inside the horseshoe region, however, the different torque distributions highlight the existence of an additional corotation torque in weakly magnetized discs. Interestingly, the additional corotation torque takes negative values in the $\sim$ inner half of the horseshoe region, and positive values in the outer half. This approximately symmetric distribution conspires to make the additional torque have a very small net amplitude, which accounts for the good agreement between the turbulent and viscous total torques shown in the right panel of Fig. 3. The properties of this new corotation torque, in particular its dependence with the strength and gradient of the background toroidal magnetic field, will be presented in a future study.

References

Baruteau, C., Fromang, S., Nelson, R. P., & Masset, F. 2011, A&A, 533, A84+
Ida, S. & Lin, D. N. C. 2008, ApJ, 685, 584
Masset, F. S. & Casoli, J. 2010, ApJ, 723, 1393
Masset, F. S., Morbidelli, A., Crida, A., & Ferreira, J. 2006, ApJ, 642, 478
Mordasini, C., Alibert, Y., Benz, W., & Naef, D. 2009, A&A, 501, 1161
Paardekooper, S., Baruteau, C., & Kley, W. 2011, MNRAS, 410, 293
Ward, W. R. 1997, Icarus, 126, 261